Pasture Appendix

Collection 9

Version 1

General coordinator
Laerte Guimarães Ferreira Jr.
Technical coordinator
Vinicius Vieira Mesquita

Team
Ana Paula Matos
Claudinei de Oliveira Santos
Ikanuza Rodrigues Pimentel de Souza
Jade Helena Plaza De Oliveira
Jairo Matos da Rocha
Lana Mara
Leandro Parente
Lucas Tales Da Silva
Luís Bauman
Mariana Gomes
Nathalia Teles
Nathaly Zaine Barcelos Silva de Brito
Pâmela Camila Assis
Renato Gomes Silvério
Roberto de Urzeda Paiva
Tharles Andrade
Wilton Ladeira da Silva

1. Overview

In the context of the information produced by MapBiomas, there are maps that describe the dynamics of land occupation by pasturelands in the last 39 years (Collection 9). This information is crucial for a better understanding of the complex processes related to changes in land use and land cover in Brazil, especially those related to the gain and loss of biodiversity and productivity.

Specifically, the MapBiomas pasture mapping has been based on the approach described in Parente *et al.* (2017) using the Landsat satellite series and the supervised classifier Random Forest with different feature space and sampling techniques (figure 1). Every collection had improvements that helped to increase the overall accuracy and to reduce the confusions between pastures and other land-cover and land-use types (e.g. native vegetation, agricultural crops).

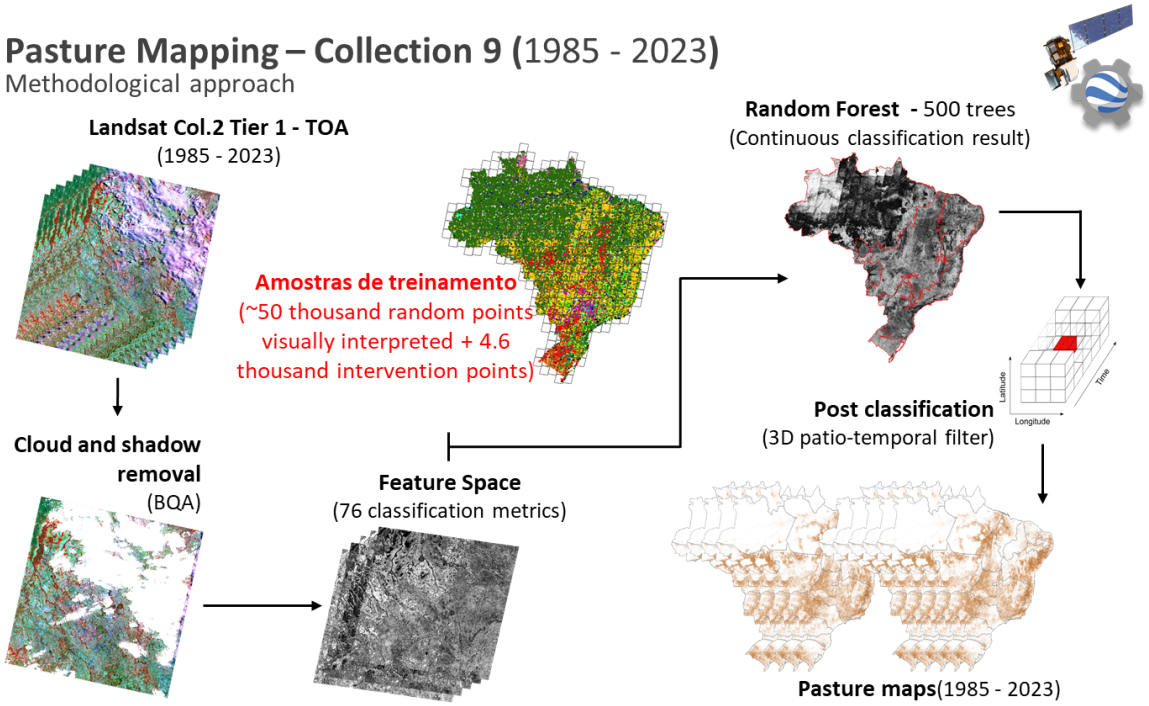

Figure 1. Pasture mapping workflow regarding the MapBiomas Collection 9.

2. Landsat image mosaics

The pasture mapping was produced with Landsat data Collection 2 Tier 1 (from 1985 to 2023) (Markham & Helder, 2012). Landsat 5 images were used in the first half of the time series (*i.e.* 1985 to 1999). The images acquired by Landsat 7 were considered only for 2000, 2001, 2002 and in 2012 (due to the failure of the *Scan Line Corrector* mechanism - Markham *et al.*, 2004). For the time periods from 2003 until 2011 and from 2013 to 2021 we used, respectively, Landsat 5 and Landsat 8 images. These time series were normalized to Top-of-Atmosphere (TOA) reflectances and screened with the Landsat Quality Assessment Band (QA = 2720 for Landsat 8 and QA = 672 for Landsat 5/7) in order to remove pixels contaminated with clouds and cloud shadows (ROY *et al.*, 2014).

2.1. Definition of the temporal period

Our mapping approach considered as a classification unit the useful limits of the Landsat scenes (according to the Worldwide Reference System - WRS-2 Path/Row without the overlapping zones) and a 24-month time window, for the entire country, ensuring the prevalence of observations of a specific year (*e.g.* the feature space of 1994 considered images of the second semester of 1993 and the first semester of 1995) (figure 2). This time window provides a denser time series for the generation of the feature space, which is capable to capture, in a more adequate way, the vegetative vigor variations of pastures, since these areas are very susceptible to climatic variations (Ferreira *et al.*, 2013).

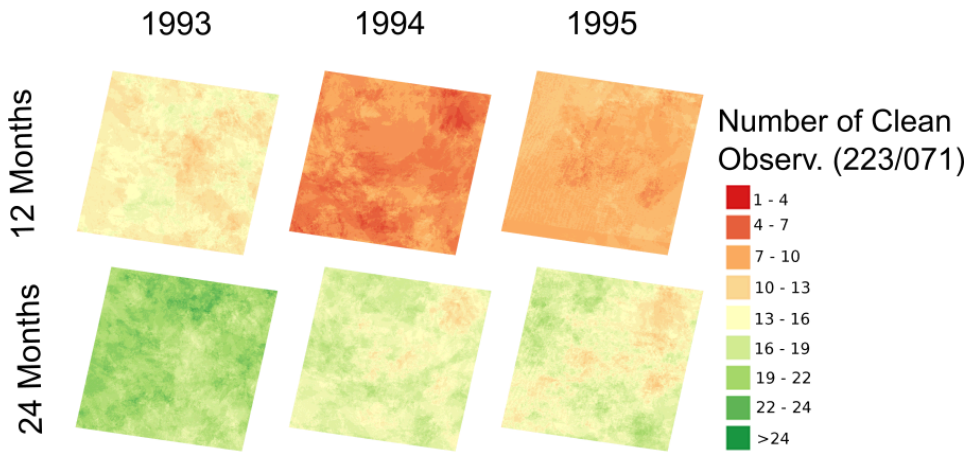

Figure 2. Number of good observations (without clouds and cloud shadows) available for the Landsat scene 223/071, considering 12 months (*i.e.* without year overlap) and 24 months (*i.e.* the 1994 image considered observations of the second half of 1993 and the first half of 1995).

2.2. Image selection

For all the "pasture" Collections generated until now, the composited Landsat images (bands and indices) utilized in the classification process were selected only for the wet season. The operationalization of this approach, a challenge for a country with continental dimensions as Brazil, occurs automatically, on a pixel basis, through a percentile analysis of all NDVI values for the assumed time window. Specifically, only observations with values greater than the NDVI 25th percentile are considered to compose the wet season, in a 24-month window. For Collection 5 onwards, the NDVI 25th percentile values were further categorized according to four other percentiles, i.e. 10, 25, 75, and 90%. Therefore, four additional radiometric bands were incorporated to the classification process concerning Collections 5, 6, and 7.

2.3 Time-series normalization

The time-series normalization aims to increase the temporal consistency of the spectral data obtained by different sensors, allowing to expand the quantity of recurrent observations obtained for the same region. Specifically for the Landsat time-series, this technique enables the use of spectral samples obtained by different sensors (*i.e.* TM, ETM+,

OLI) in the same training process utilized by the machine learning algorithms (Chavez & Mackinnon,1994; Roy *et al.*, 2016).

In this direction, we tentatively implemented in Collection 4, a relative calibration method (Furby & Campbell, 2001) between the data obtained by the ETM+ and OLI sensors, which produced a Landsat 7 pixel value corrected for Landsat 8, considering all images obtained between 2013 and 2017 (figure 3). The Landsat 7 images were aligned with the Landsat 8 images, assuming that the eight days difference between the acquisition of the two images does not significantly impact the normalization process. For each WRS Landsat in Brazil, and for each spectral band, a regression was trained using the SVM algorithm and the same sample points used in the classification algorithm (see section 3.3). Only samples without land use and land cover change, between 2013 and 2017, were considered in the regression. The entire process was implemented on Google Earth Engine (https://code.earthengine.google.com/5c09817f5926b2efca0506bfb8c465fc) and resulted in 1,900 regressions (*i.e.* 381 WRS Landsat and 5 spectral bands). The regressions were applied in their respective scenes and spectral bands in all Landsat 5 and 7 images used in Collection 4 obtained between 1985 and 2012. Although there are differences between TM and ETM+ sensors, we used the same regression for both sensors based on their spectral similarity.

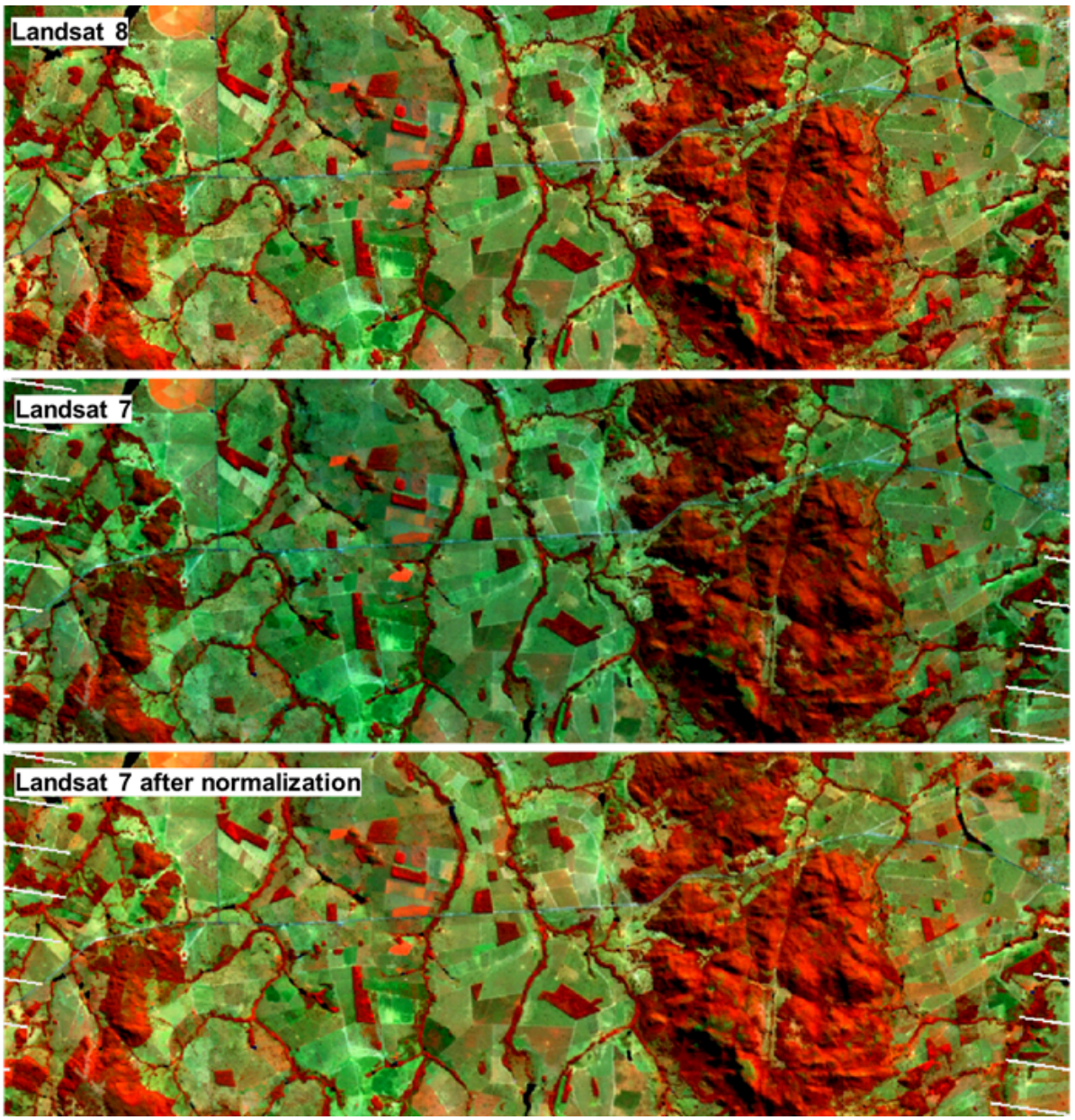

Figure 3. Color composition comparison between Landsat 8 and Landsat 7 images, before and after normalization (such normalization attempt was implemented only in Collection 4).

3. Classification

The classification approach considers a set of metrics that encompass the spectral variations, along a time window, to capture the seasonal characteristics of one or more land use and land cover classes (WANG *et al*., 2015; Pasquarella *et al*., 2018). These metrics are used to create a feature space, which is classified via the Random Forest algorithm (Breiman, 2001) calibrated with 31,449 training points (visually inspected and randomly distributed throughout the Brazilian territory). This section presents the progress regarding our pasture mapping approaches, whose rationale are thoroughly discussed in the following papers: Parente *et al.*, 2017, Parente & Ferreira, 2018, e Parente *et al*., 2019.

3.1. Classification scheme

Stratified classification approaches allow machine learning algorithms to be trained to capture geographic and temporal aspects specific to one, or more, land use and land cover classes. However, its correct application depends on the existence of training samples for each stratum. Multitemporal classifications, for example, need samples that represent each defined period in time (*e.g.* years). On the other hand, it is possible to use a single model to classify the entire time series, once that time-series data were normalized.

3.1.1. Geographical and temporal stratification

Our classification scheme considers a geographical and temporal stratification, in which all the 381 Landsat scenes necessary to encompass the entire Brazilian territory are individually trained and classified, on an annual basis, since 1985. Considering that pastures areas are very susceptible to climatic inter-annual variations (Ferreira *et al*., 2013) and present different biophysical and management characteristics throughout Brazil (Aguiar *et al*., 2017; Ferreira *et al*., 2013b), this approach allows the classification models to better perform regarding the identification of the pasture class. However, to minimize the impact of geographical stratification, part of the training samples is shared across different classification models. In practice, 900 points are used to train a specific model for one scene, with a total of 800 points recovered from the immediately adjacent scenes.

3.1.2. Only geographical stratification for Landsat 8 time-series

The classification approach for the years after 2017 (*i.e*. regarding Collections 4, 5, 6, and 7) utilizes samples from five years, considering only the monitoring period of Landsat 8 and assuming that the trained classifier is able to handle the spectral interannual variations of the earth's surface. This approach eliminates the need for new training samples every year and allows greater variability in the samples, as it contains higher seasonality conditions. Other aspects of the classification approach are kept according to Collection 3, including the sample balancing, that is proportional to the pasture area of each WRS Landsat. Specifically, for Collections 4 and 5, the 2018 and 2019 images, respectively, were classified based on samples from years 2017, 2016, 2015, 2014, and 2013. For Collection 6, even though the yearly sample dataset was updated until 2020, the same sample generalization logic was considered. Thus, for Collection 6, released in 2021, the 2018, 2019, and 2020 images were classified based on samples from 2016, 2017, 2018, 2019, 2020. For the Collection 7 (released in August, 2020) the same idea was applied to the 2021 images.

Specifically for Collection 8, an entire revision over the 31 thousand training samples, from 1985 to 2022, was conducted, and another 19 thousand new training samples included. In addition, 4.296 new training samples were added as intervention points to specific situations where the classifier was performing poorly to map pasturelands or mapping non-pasture areas wrongly. Also, for Collection 9, the year 2023 was included and the last 3 years (2020 - 2022) were reviewed to keep the consistency of the land cover classes.

3.2. Feature space

On the Landsat images filtered with the BQA (Band Quality Assessment Aand) and selected according to the established time window (section 2.1. Definition of the temporal period), five operations are applied (*i.e.* mean, standard deviation, minimum, maximum, amplitude and percentiles) over six spectral bands (*i.e.* green, red, near-infrared, shortwave infrared 1 and shortwave infrared 2) and three spectral indices (*i.e.* Normalized Difference Vegetation Index - NDVI, Normalized Difference Water Index - NDWI; Gao, 1996, and the Cellulose Absorption Index - CAI; Nagler *et al.*, 2003). The Landsat temperature band is not included as a covariate in our classification scheme due to the occurrence of saturated pixels over several dates and regions of the country. Beginning with Collection 5, we added information (Elevation and Slope) derived from the SRTM Digital Elevation Model (DEM) and geographic coordinates. In total, our pasture mapping for Collections 3 and 4 used 40 spectral-temporal bands and, for Collections 5, 6, 7, 8 and 9, 72 spectral-temporal bands and four spatial metrics (table 1).

Table 1. Feature space utilized for the pasture classification in Collections 3 to 9, considering 72 spectral-temporal and four spatial metrics.

#	Bands / indices	Operation	"Season"	Collection
1	Green	Mean	WET	3, 4, 5, 6, 7, 8 and 9
2	Green	Standard Deviation	WET	3, 4, 5, 6, 7, 8 and 9
3	Green	Minimum	WET	3, 4, 5, 6, 7, 8 and 9
4	Green	Maximum	WET	3, 4, 5, 6, 7, 8 and 9
5	Green	Amplitude	WET	3, 4, 5, 6, 7, 8 and 9
6	Green	Percentile 10%	WET	5, 6, 7, 8 and 9
7	Green	Percentile 25%	WET	5, 6, 7, 8 and 9
8	Green	Percentile 75%	WET	5, 6, 7, 8 and 9
9	Green	Percentile 90%	WET	5, 6, 7, 8 and 9
10	Red	Mean	WET	3, 4, 5, 6, 7, 8 and 9
11	Red	Standard Deviation	WET	3, 4, 5, 6, 7, 8 and 9
12	Red	Minimum	WET	3, 4, 5, 6, 7, 8 and 9
13	Red	Maximum	WET	3, 4, 5, 6, 7, 8 and 9
14	Red	Amplitude	WET	3, 4, 5, 6, 7, 8 and 9
15	Red	Percentile 10%	WET	5, 6, 7, 8 and 9
16	Red	Percentile 25%	WET	5, 6, 7, 8 and 9
17	Red	Percentile 75%	WET	5, 6, 7, 8 and 9
18	Red	Percentile 90%	WET	5, 6, 7, 8 and 9
19	NIR	Mean	WET	3, 4, 5, 6, 7, 8 and 9
20	NIR	Standard Deviation	WET	3, 4, 5, 6, 7, 8 and 9

21	NIR	Minimum	WET	3, 4, 5, 6, 7, 8 and 9
22	NIR	Maximum	WET	3, 4, 5, 6, 7, 8 and 9
23	NIR	Amplitude	WET	3, 4, 5, 6, 7, 8 and 9
24	NIR	Percentile 10%	WET	5, 6, 7, 8 and 9
25	NIR	Percentile 25%	WET	5, 6, 7, 8 and 9
26	NIR	Percentile 75%	WET	5, 6, 7, 8 and 9
27	NIR	Percentile 90%	WET	5, 6, 7, 8 and 9
28	SWIR1	Mean	WET	3, 4, 5, 6, 7, 8 and 9
29	SWIR1	Standard Deviation	WET	3, 4, 5, 6, 7, 8 and 9
30	SWIR1	Minimum	WET	3, 4, 5, 6, 7, 8 and 9
31	SWIR1	Maximum	WET	3, 4, 5, 6, 7, 8 and 9
32	SWIR1	Amplitude	WET	3, 4, 5, 6, 7, 8 and 9
33	SWIR1	Percentile 10%	WET	5, 6, 7, 8 and 9
34	SWIR1	Percentile 25%	WET	5, 6, 7, 8 and 9
35	SWIR1	Percentile 75%	WET	5, 6, 7, 8 and 9
36	SWIR1	Percentile 90%	WET	5, 6, 7, 8 and 9
37	SWIR2	Mean	WET	3, 4, 5, 6, 7, 8 and 9
38	SWIR2	Standard Deviation	WET	3, 4, 5, 6, 7, 8 and 9
39	SWIR2	Minimum	WET	3, 4, 5, 6, 7, 8 and 9
40	SWIR2	Maximum	WET	3, 4, 5, 6, 7, 8 and 9
41	SWIR2	Amplitude	WET	3, 4, 5, 6, 7, 8 and 9
42	SWIR2	Percentile 10%	WET	5, 6, 7, 8 and 9
43	SWIR2	Percentile 25%	WET	5, 6, 7, 8 and 9
44	SWIR2	Percentile 75%	WET	5, 6, 7, 8 and 9
45	SWIR2	Percentile 90%	WET	5, 6, 7, 8 and 9
46	NDVI	Mean	WET	3, 4, 5, 6, 7, 8 and 9
47	NDVI	Standard Deviation	WET	3, 4, 5, 6, 7, 8 and 9
48	NDVI	Minimum	WET	3, 4, 5, 6, 7, 8 and 9
49	NDVI	Maximum	WET	3, 4, 5, 6, 7, 8 and 9
50	NDVI	Amplitude	WET	3, 4, 5, 6, 7, 8 and 9
51	NDVI	Percentile 10%	WET	5, 6, 7, 8 and 9
52	NDVI	Percentile 25%	WET	5, 6, 7, 8 and 9
53	NDVI	Percentile 75%	WET	5, 6, 7, 8 and 9
54	NDVI	Percentile 90%	WET	5, 6, 7, 8 and 9
55	NDWI (Gao, 1996)	Mean	WET	3, 4, 5, 6, 7, 8 and 9

56	NDWI (Gao, 1996)	Standard Deviation	WET	3, 4, 5, 6, 7, 8 and 9
57	NDWI (Gao, 1996)	Minimum	WET	3, 4, 5, 6, 7, 8 and 9
58	NDWI (Gao, 1996)	Maximum	WET	3, 4, 5, 6, 7, 8 and 9
59	NDWI (Gao, 1996)	Amplitude	WET	3, 4, 5, 6, 7, 8 and 9
60	NDWI (Gao, 1996)	Percentile 10%	WET	5, 6, 7, 8 and 9
61	NDWI (Gao, 1996)	Percentile 25%	WET	5, 6, 7, 8 and 9
62	NDWI (Gao, 1996)	Percentile 75%	WET	5, 6, 7, 8 and 9
63	NDWI (Gao, 1996)	Percentile 90%	WET	5, 6, 7, 8 and 9
64	CAI (Nagler *et al.*, 2003)	Mean	WET	3, 4, 5, 6, 7, 8 and 9
65	CAI (Nagler *et al.*, 2003)	Standard Deviation	WET	3, 4, 5, 6, 7, 8 and 9
66	CAI (Nagler *et al.*, 2003)	Minimum	WET	3, 4, 5, 6, 7, 8 and 9
67	CAI (Nagler *et al.*, 2003)	Maximum	WET	3, 4, 5, 6, 7, 8 and 9
68	CAI (Nagler *et al.*, 2003)	Amplitude	WET	3, 4, 5, 6, 7, 8 and 9
69	CAI (Nagler *et al.*, 2003)	Percentile 10%	WET	5, 6, 7, 8 and 9
70	CAI (Nagler *et al.*, 2003)	Percentile 25%	WET	5, 6, 7, 8 and 9
71	CAI (Nagler *et al.*, 2003)	Percentile 75%	WET	5, 6, 7, 8 and 9
72	CAI (Nagler *et al.*, 2003)	Percentile 90%	WET	5, 6, 7, 8 and 9
73	SRTM (Farr *et al.*, 2007)	Elevation	-	5, 6, 7, 8 and 9
74	SRTM (Farr *et al.*, 2007)	Slope	-	5, 6, 7, 8 and 9
75	Geographic Coordinate	Latitude	-	5, 6, 7, 8 and 9
76	Geographic Coordinate	Longitude	-	5, 6, 7, 8 and 9

3.3. Classification algorithm, training samples and parameters

The mapping approach used in Collections 3 and 4 considered the same feature space, training samples and machine learning algorithm (*i.e.* Random Forest), modifying only the stratification strategy and sample balancing in the classification process. For Collection 5 onward, we use a similar approach as in Collection 4, with the difference being only the increment of new metrics in the feature space (table 1).

3.3.1. Collection 3

The collection 3 classification approach uses the Random Forest algorithm (Breiman, 2001), which demands training samples. Considering the absence of reference data, spatially explicit, for the entire mapping period, we decided to produce a training dataset with 31,449 points, randomly distributed over Brazil (figure 4), ensuring 100 points for each

Landsat scene. Nevertheless, in the border scenes, with the ocean and neighboring countries, this amount was weighted by the respective Brazilian territory area of the scene. The sampling design used the pasture map of 2015 (Parente *et al*., 2017) to reflect the actual pasture area proportion, scene by scene, in the training dataset. However, for scenes with a proportion of less than 10%, a minimum amount of 10 points was randomly selected over the pasture areas.

All training samples were visually inspected by three trained interpreters, who analyzed, for each point, two Landsat images per year, regarding the dry and wet periods, classifying, for 33 years, each transition according to 10 land cover and land use classes (*i.e.* pasture, crop agriculture, planted forest, native vegetation, mixed use, water bodies, urban area, mining, and others). This assessment was conducted using the Temporal Visual Inspection Tool (Nogueira *et al*., 2017; Parente et al., 2021), which also considers the respective MOD13Q1 NDVI time series and high-resolution Google Earth images (figure 5). The Random Forest used 500 statistical decision trees to associate a per pixel pasture probability. For example, a pixel with a pasture probability of 60% had 300 trees indicating the pasture class and 200 trees the non-pasture class.

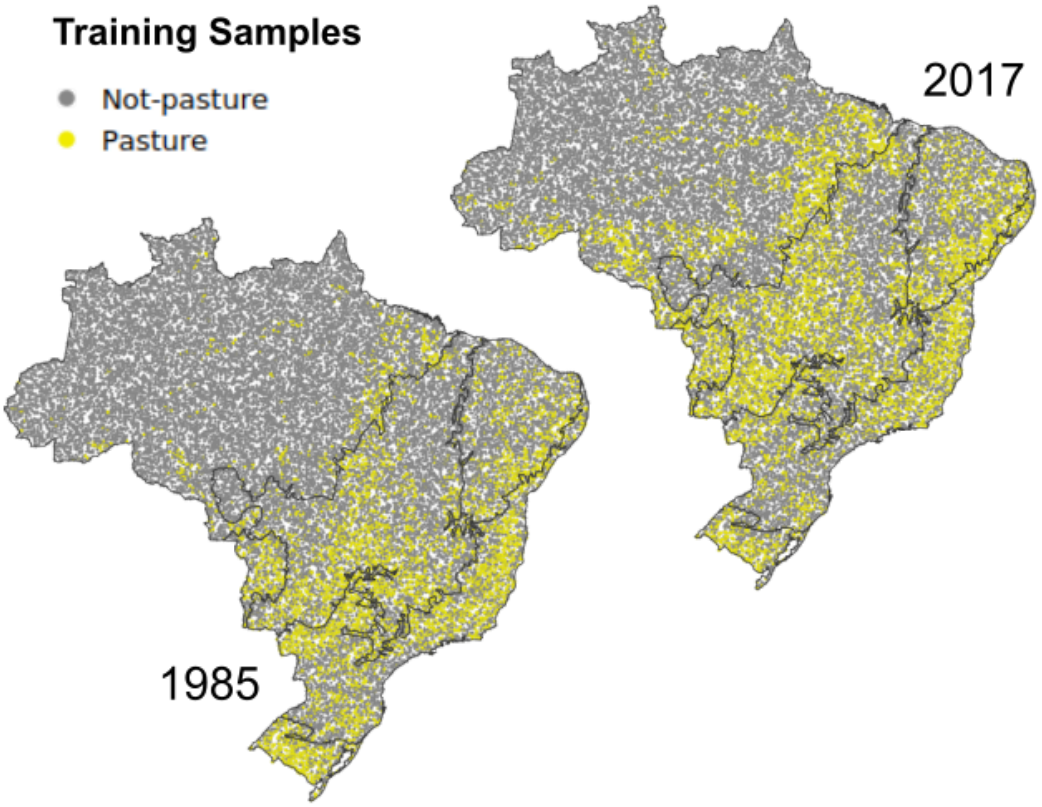

Figure 4. Training samples with the consolidated classes, assigned by the visual inspection, between 1985 and 2017 (Collection 3). Each one of the 31,449 points was inspected by three interpreters[1] [2].

[1] For Collection 6 (and 7) this point collection was updated, comprising now the period from 1985 to 2020.

[2] For Collection 8 this point collection was updated with an addition of 18,550 randomly stratified points and 4,664 intervention points, comprising now the period from 1985 to 2022 and a total amount of 54,663 samples.

Figure 5. Temporal Visual Inspection tool (TVI) allows users to visualize two Landsat images, regarding the dry and wet seasons, as well as a MOD13Q1 NDVI time series. This image is located in Luís Eduardo Magalhães - BA.

3.3.2. Collection 4

Collection 4 used only the geographical stratification approach (see section 3.1.3), considering a different sample balancing from Collection 3. In this direction, a single classifier was trained using 15,000 samples distributed from 1985 to 2017, considering balanced samples (*i.e.* 50% pasture and 50% not-pasture). Not-pasture samples were organized locally and globally. Local samples were obtained using the logic of neighboring scenes, according to Collection 3 (see section 3.1.1.), considering all available years and the crop agriculture, planted forest, and native vegetation classes. The global samples were obtained considering the entire Brazilian territory and were shared among all trained classifiers, considering all available years and the classes of water bodies, urban areas and sand banks, which have similar spectral characteristics throughout the surface. For pasture samples only local samples were used and for Random Forest the parameters of Collection 3 were maintained (see section 3.3.1).

3.3.3. Collection 5

Aiming to reduce the computational cost and the commission errors observed in Collection 4, Collection 5 used the same stratification approach as Collection 3 from 1985 to 2017 (see section 3.1.1) and the geographical and temporal approach (see section 3.1.2) from 2018. The main difference between Collections 5 and 3 is the increment of new spectral-temporal metrics derived from the percentiles 10%, 25%, 75% and 90% (considering only values above the “original” 25 percentile), which proved to be very helpful to distinct land use types (Zalles *et al*., 2019), once it aggregates information regarding the intra annual spectral behavior. Likewise, spatial metrics like elevation and slope, derived by the Digital Elevation Model (DEM) produced by the Shuttle Radar Topography Mission - SRTM (Farr *et al.*, 2007), and geographic coordinates, have been added to improve the spatial learning capacity of the classifier. The metrics were chosen based on the results of multiple classifier performance tests that shows an improvement in the classifier accuracies scene by scene (figure 6) compared to the same test with Collection 3 metrics. This test was performed in R language (R Core Team, 2020) with the randomForest classifier package (Liaw and Wiener, 2002) and the K-Fold Cross-Validation algorithm from Caret package (Kuhn ,2008; Caret, 2020). This test also used the same samples, metrics and parameters used in the pasture mapping via Google Earth Engine.

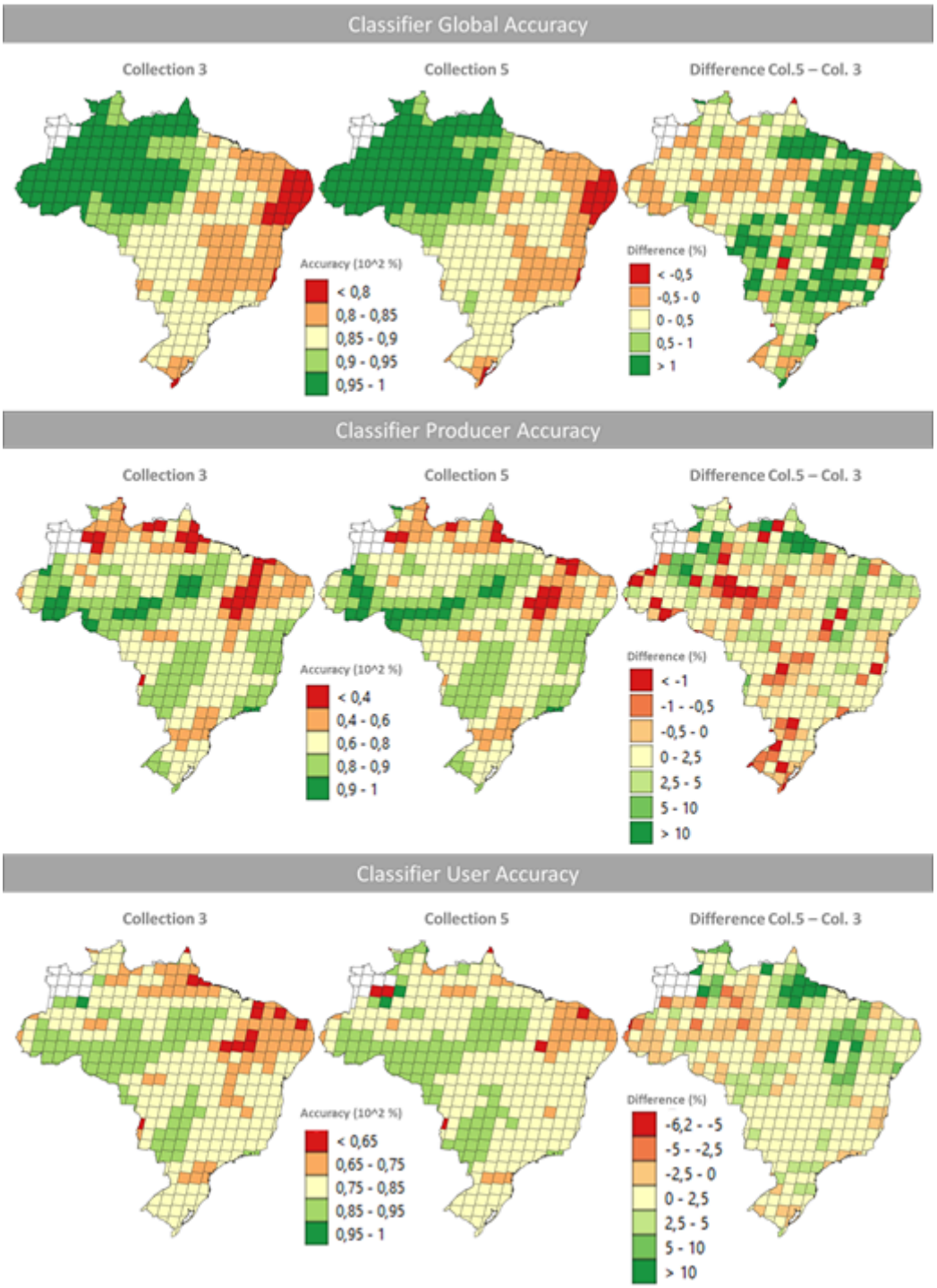

Figure 6. Comparison between the classifier accuracies (scene by scene) reached by the metrics of Collections 3 and 5. The improvements in the classifier performance and capacity to map pasture using the metrics utilized in Collection 5 was significant when compared with Collection 3.

The codes used to produce Collection 5 are available at [MapBiomas Github repository](#).

3.3.4. Collection 6

The production of this collection was focused on ensuring the continuity of training and validation samples for the pasture mapping from 2018 to 2020, while considering the same mapping approach adopted in Collection 5. The samples were inspected by two experts using a strategy TVI-like based on the GIS software QGIS with the Earth Engine Package (see 3.3. Classification algorithm, training samples and parameters) for the years 2018 to 2020.

3.3.5. Collection 7

Two distinct mapping approaches were considered in the production of Collection 7. First, a similar one (named 7B) to that adopted in Collection 6, thus ensuring, in a straightforward manner, the pasture mapping continuity from 1985 to 2021. In parallel, a more sophisticated strategy (named 7A), considering additional context information, was evaluated. Specifically, in the approach 7A the classification algorithm was calibrated based on the set of covariates associated with both a given training point, as well as to the eight surrounding pixels (figure 7)[3].

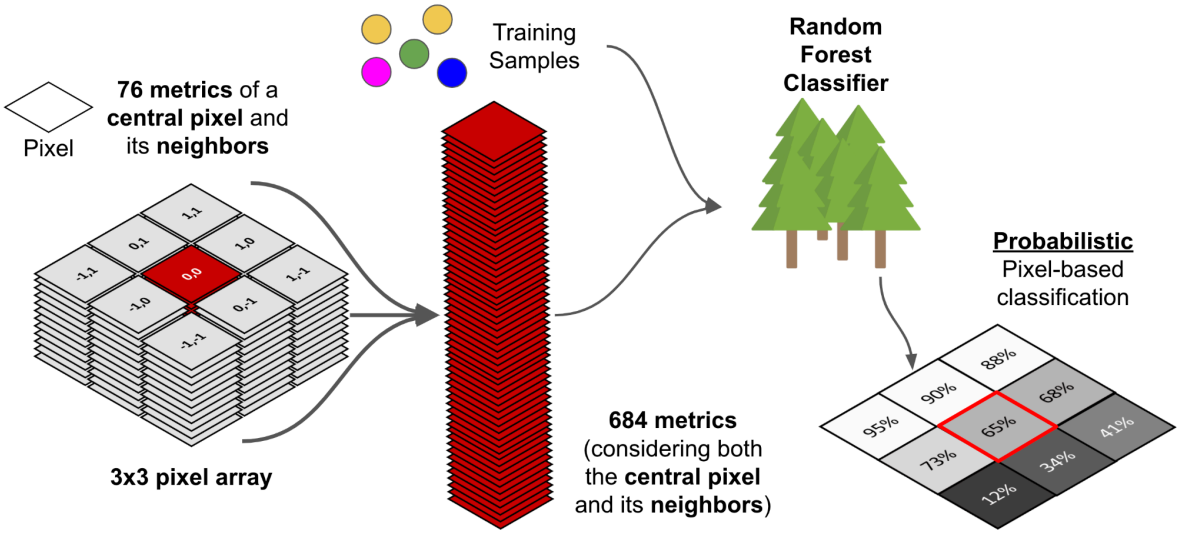

Figure 7. Use of context information evaluated in Collection 7.

Given that the "surrounding" approach led to reduced pasture areas, particularly within the Cerrado and Caatinga biomes after 2016, we opted for the more conventional "7B" approach for the operational production of Collection 7 pasture maps. Until a more comprehensive evaluation can be conducted to determine the potential impacts, regarding both commission and omission errors that might arise due to the increased set of covariates from neighboring pixels, we decided not to use the approach "7A".

[3] The codes used to produce Collection "7A" (evaluation version) are available at MapBiomas Github repository.

3.3.6. Collection 8

For Collection 8, the entire set of training samples (~31 thousand samples) used to do the pasture mapping was reviewed from 1985 to 2022 and another set of 19 thousand new samples was inspected for the same period (Figure 8). The assumption here was that Increasing the amount of training samples improves the classifier performance, by increasing the representativeness of pasture and non-pasture variability. Also, for specific cases, intervention training samples were added focusing on solving local mistakes or confusion of the classifier.

Figure 8. Training samples used in the Pasture Mapping on Collection 8.

3.3.7. Collection 9

During processing of pasture maps of collection 9, tests were performed using cubic Savitzky-Golay filters with 3x3x3 (3x3 pixels and 3 years) and 5x5x5 (5x5 pixels and 5 years) windows. These filters were applied to the map series in order to obtain substantial improvements over the multidimensional median filter (3x3x5) used in the past collections. However, no significant improvements or changes were observed between the results and the Savitzky-Golay filter results showed a tendency to increase the commission of cropland area.

4. Post-classification

As all maps are produced year by year and independently, a post-classification approach is used to increase the temporal and spatial consistency of the final result.

4.1. Spatial-temporal filter (3x3x5)

All the classified scenes are retrieved from Google Drive and merged, on a yearly basis, thus producing a time series of probability pasture maps (see 3.3. Classification algorithm, training samples and parameters). To improve these results, we apply a space-time filter, capable of minimizing abrupt, and sometimes unreal, transitions, simultaneously using information from these two dimensions. The filter, implemented through the SciPy library (Scipy, 2018), uses a 5-year time window and 3 x 3 pixels to replace the central kernel value with the median of 45 probability values (figure 9). Upon this result, a threshold of 51% is applied as a minimal acceptable value to confirm the pixels's classification to produce the pasture maps for Brazil.

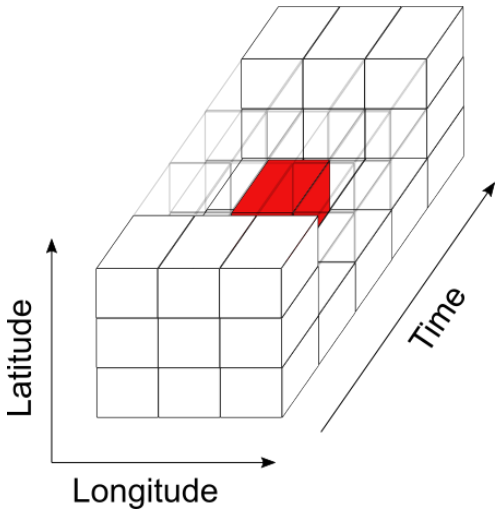

Figure 9. The kernel, with 3x3 pixels and 5 years, is used in the space-time filtering of the probability pasture maps produced with Random Forest. The central pixel, highlighted in red, is replaced by the median of the probabilities of the 45 pixels kernel.

5. Validation strategies

We perform an independent quality assessment considering 5,000 validation points (figure 10), as well as 1,225 points collected in the field by multiple institutions and initiatives (figure 11). The validation sampling design also considered a pasture map of 2015 (Parente *et al*., 2017), so that the number of random points could be balanced per class (*i.e.* 2,500 for the "pasture" class and 2,500 for the "not-pasture"), conservatively assuming the minimum mapping accuracy is 50% and the error of accuracy assessment is 1% within a 95% confidence interval (Lohr, 2009).

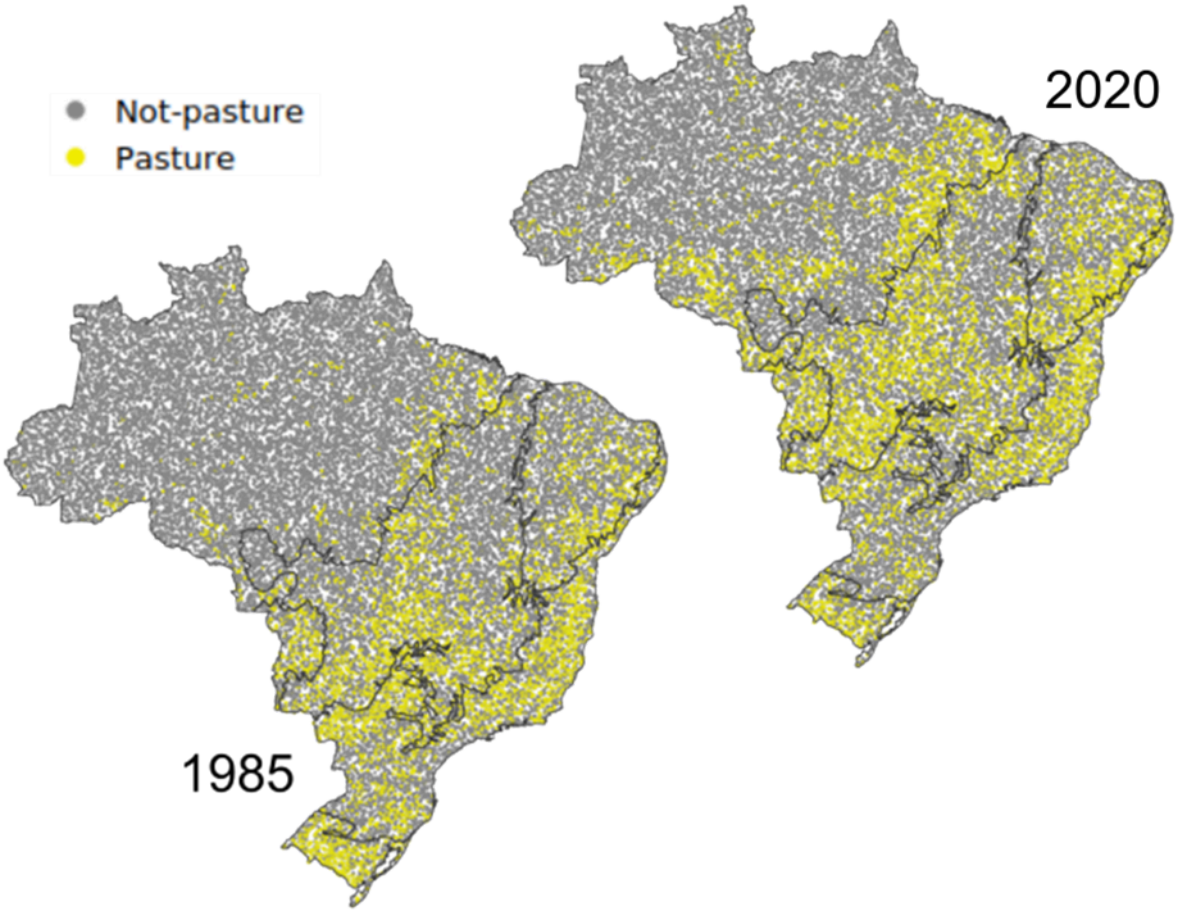

Figure 10. Validation samples with the consolidated classes, assigned through visual inspection, in the years of 1985 and 2020. Each of the 5,000 points was inspected by five interpreters.

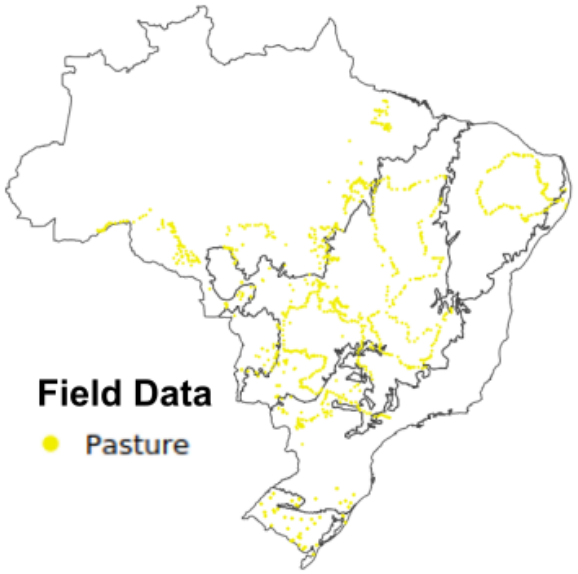

Figure 11. Field data, equivalent to 1,225 points, collected by LAPIG/UFG, Embrapa, TNC, Aliança da Terra, Rally da Pecuária, Associação de Plantas do Nordeste (APNE),

Universidade Estadual de Feira de Santana (UEFS), Universidade Federal do Rio Grande do Sul (UFRGS), and WWF, between 2014 and 2018.

The validation samples were inspected by five interpreters, but only points with agreement of four or more votes were considered in the accuracy assessment (*i.e.* at least four interpreters identified the same land cover and land use class), resulting in (at least) 4,100 samples available for each year. For all the pasture maps, the global, producer and user accuracies were assessed with a balanced confusion matrix, which removes sampling bias (Pontius & Millones, 2011).

The pasture maps present an overall accuracy of ~91%, an user accuracy of ~95% (from 2000 on), and a producer accuracy varying between 60% and 72%, indicating a prevalence of omission errors in all years (figure 12). With the gradual decrease of omission errors in recent years, this assessment reveals that the most accurate, and recent, pasture map is for the year 2015. In Collections 3 and 4, the decay of producer accuracy in the years 2016 and 2017 can be explained by the lack of information, after 2017, for the space-time filter. For the decay observed in Collection 5, the possible cause is inherited information from maps of 2018 and 2019 (generated using the approach described in section “3.1.2”, and without the time series normalization).

The evaluation using field data, obtained between 2013 and 2018, was performed only with the 2015 pasture map, which mapped 984 of 1225 pasture field points in Collection 3, 1048 in Collection 4 and 988 in Collection 5, corresponding to accuracies of 80.32%, 83.50% and 80,65%, respectively. This accuracy rate, greater than the producer's accuracy performed with validation samples, can be explained by the spatial distribution of the field samples, collected in pasture areas more consolidated and relevant to livestock. It is important to mention that the higher producer accuracy observed for Collection 4, compared to the other collections, had an increase in the commission errors.

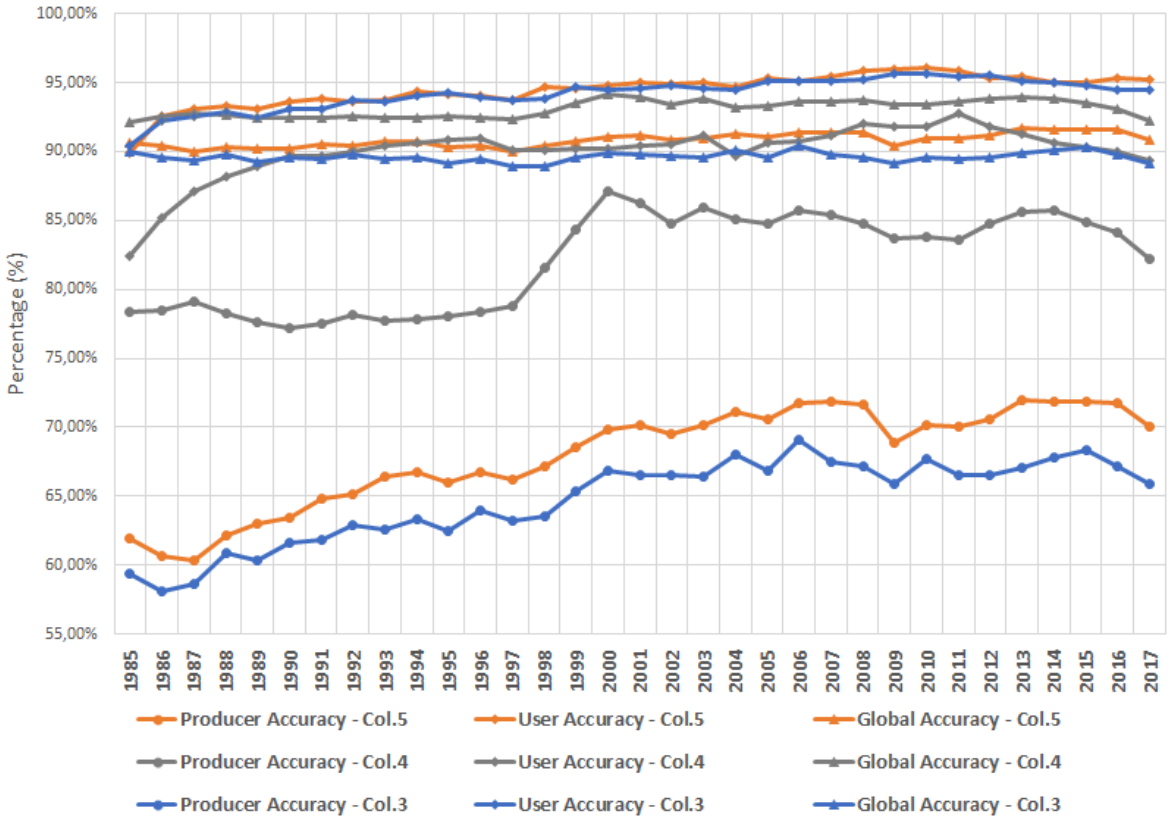

Figure 12. Accuracy assessment results for all the years (and Collections), calculated based on the validation samples, only considering points with four or more votes (*i.e.* at least four interpreters identified the same land cover and land use class).

6. Data Analysis

One of the motivations for producing a new map collection every year is to generate more spatially and temporally accurate maps for every version. Occasionally, we need to take a step back in an approach to ensure a more realistic map. For Collection 5 (as well as for Collections 6 and 7), we chose a more conservative map approach, with as little commission error as possible. Thus, we did not compare Collections 4 with 5, as the results were similar to the comparison between Collections 3 and 4.

6.1. Comparison between Collections 3 and 4

The main methodological difference between Collections 3 and 4 was the use of a single classification model for the entire time series (see section 3.1.3) combined with a sample balancing of 50-50% (see section 3.3.4). Analyzing the results of the two collections we observed the following aspects:

- The methodology of Collection 4 allowed the classification of periods without samples (*i.e.* year 2018), which allowed the use of a larger number of samples and consequently different sample balancing strategies;
- Collection 4 filled the pasture areas better, producing a map with better spatial consistency (figure 13) and lower omission error (figure 12).

- Collection 4 promoted a better separation of agricultural areas that were classified as pasture in Collection 3;
- The commission error increased in Collection 4 (figure 12), mainly due to the erroneous classification of natural areas with large spacing between trees, especially in the Cerrado and Caatinga biomes;
- Collection 4 showed a sudden increase in producer accuracy, between 1997 and 2001, probably caused by the smaller number of available observations between 1985 and 2000 (Figures 14 and 15).

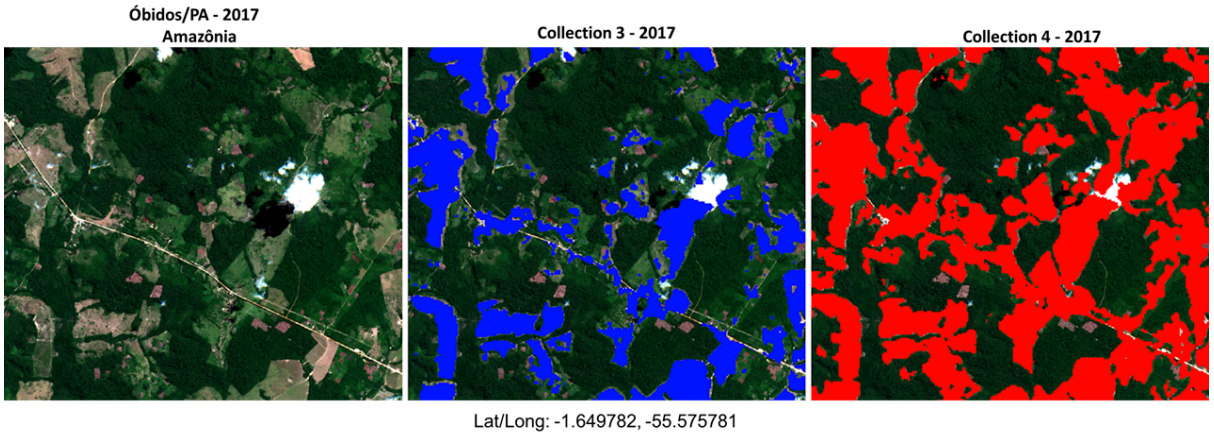

Figure 13. Examples of pasture areas for the year of 2017, for the municipality of Óbidos/Pará, as depicted by Collections 3 (blue) and 4 (red).

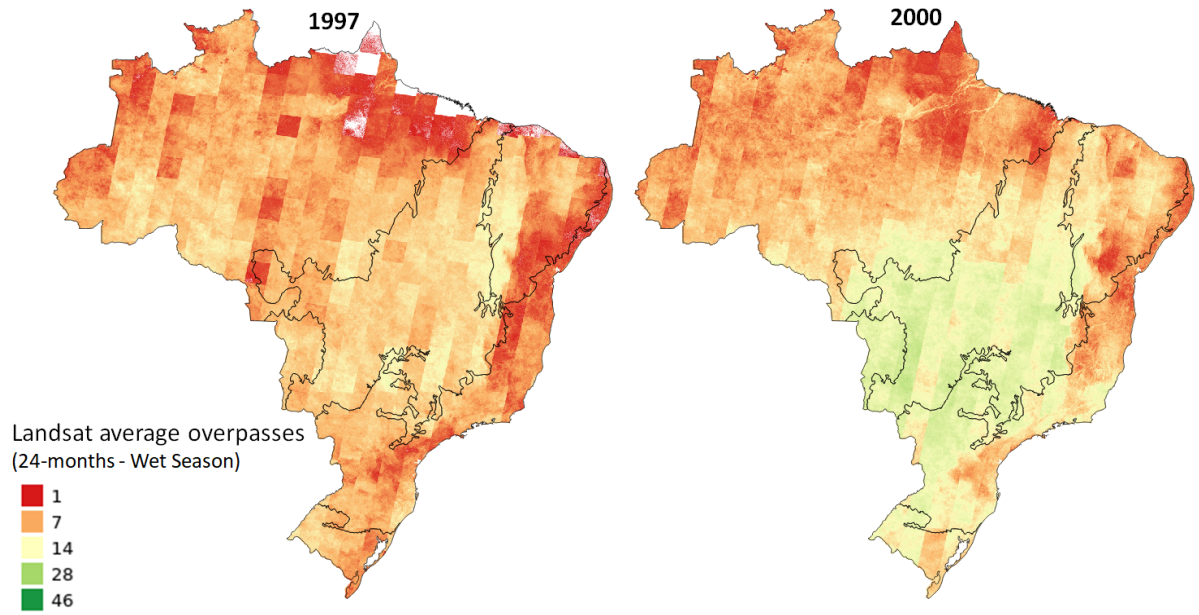

Figure 14. Number of good observations (*i.e.* without cloud and cloud shadows, for two specific years, considering the same time window used in the classification approach of Collections 3 and 4.

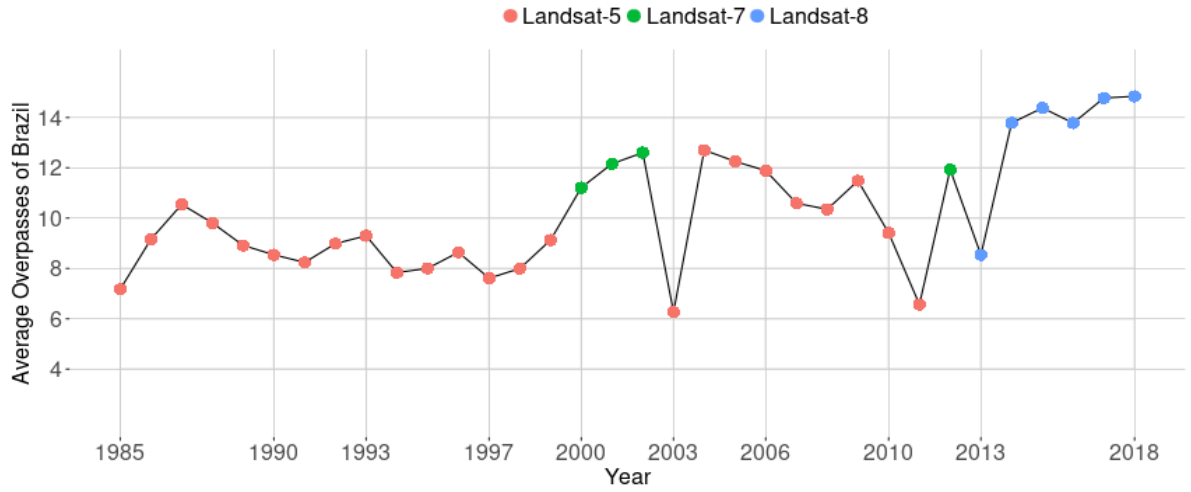

Figure 15. Average image availability per year for the entire Brazil.

6.2. Comparison between Collection 3 and 5

From 1985 to 2017, the approach used in Collection 5 (see section 3.1.3) differs from the Collection 3 only by the number of metrics used to produce the series of maps; and, from 2018 on, the classification approach, scene by scene, used only the samples available from the Landsat 8 satellite (see section 3.1.2). Analyzing the results for Collections 3 and 5 we observed the following aspects:

- The use of percentile metrics in Collection 5 helped to minimize commission error of planted forest and crop, because these metrics gave more information about the intra annual behaviors of the surface during the mapped period (24 months). The result was a more refined map compared to Collection 3 (figure 16);
- Collection 5, when compared to Collection 3, reduced the omission errors and had little impact on commission errors (figures 17 and 18). In addition, the accuracy graphic, on a yearly basis, was slightly smoother than in Collection 3 (figure 12).
- In some biomes, like Caatinga and Atlantic Forest, it was possible to observe some omission errors caused by sazonality interference, high landscape fragmentation and insufficient training samples.

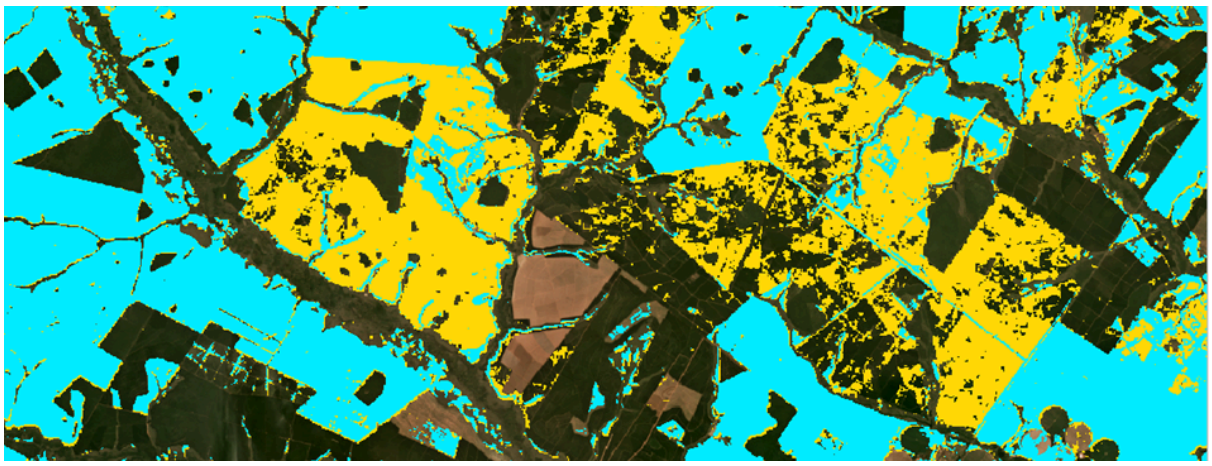

Figure 16. Mapping examples of pasture areas, for the municipality of Brasilândia/Mato Grosso do Sul, in Collections 3 (yellow) and 5 (cyan). In some cases, Collection 3 misclassified planted forest as pasture (since after the cut, grass can grow over these areas).

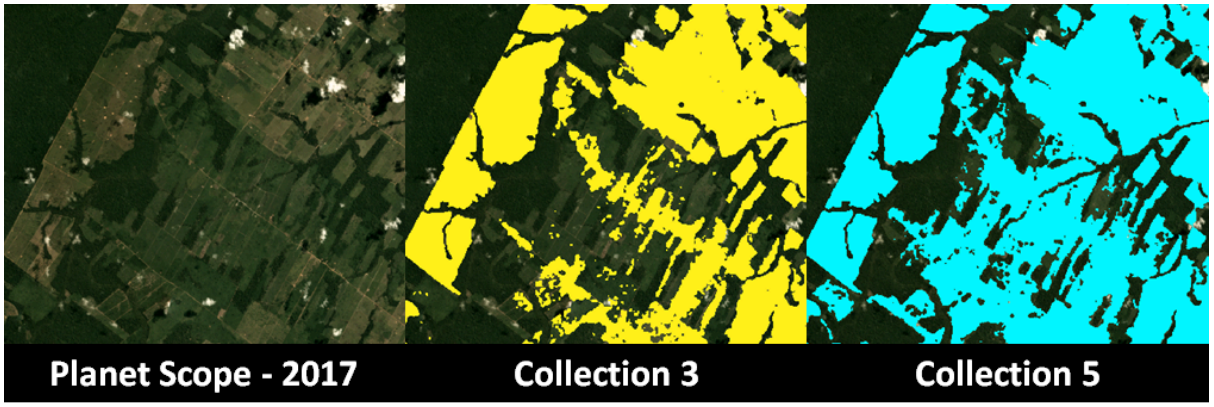

Figure 17. Mapping examples of pasture areas near Mapinguari National Park (Porto Velho/Rondônia), in Collections 3 and 5. This example shows a better pasture area (piquet) filling by Collection 5.

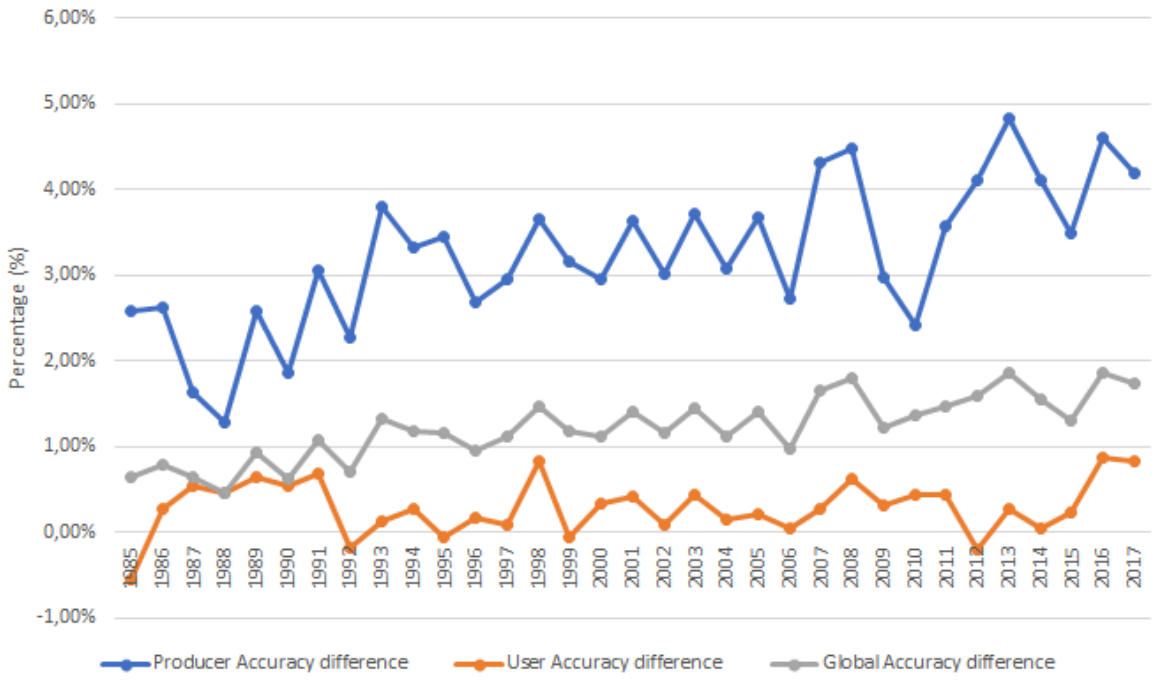

Figure 18. Differences in accuracies between Collections 5 and 3. The inclusion of new metrics helped to increase the correctly mapped pasture area over the series of maps without impacting the commission error.

6.3. Comparison between Collection 5 and 6

The modifications and updates made in Collection 6 significantly improved the differentiation between pasture areas and crop plantations, while increasing the sensibility to detect natural riparian forests inside the pasture paddocks, mainly in the Cerrado, Amazon, and Atlantic Forest biomes. The map consistency improved due to the updating of training samples and caused a reduction in the total pasture area mapped in the final maps of the series (figure 19), which was expected to happen.

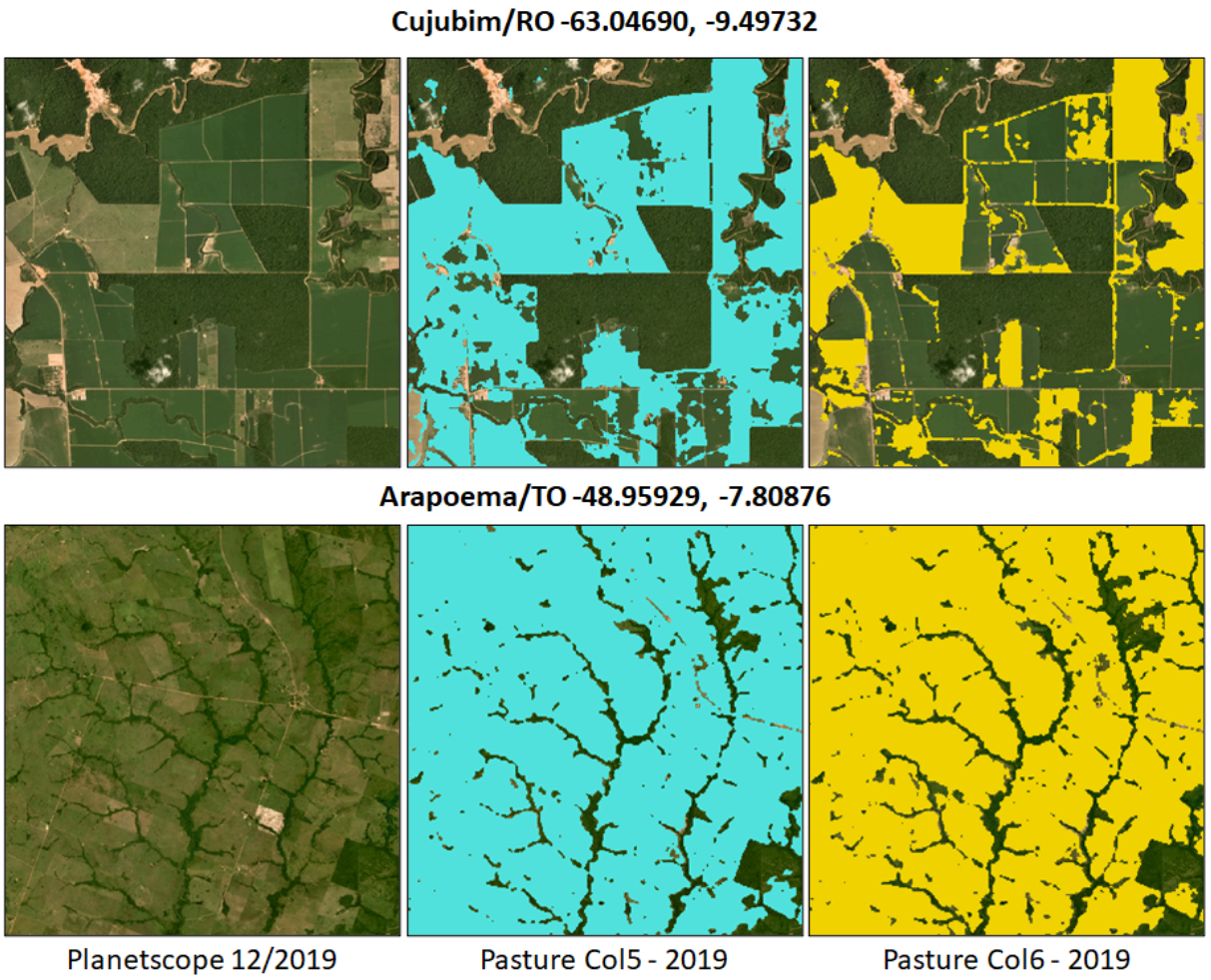

Figure 19. Improvements in Collection 6 compared to Collection 5. The updates in the training sample series enable a better differentiation between pasture and crop plantation. Also, the sample update slightly enhanced the edges between pasture and riparian forests.

6.4. Comparison between Collection 7 and 8

The increased amount of training samples and the usage of intervention samples helped to substantially improve the accuracies of the maps in Collection 8 at the cost of increasing the commission errors by an average of 0,3% (Figure 20). This newer collection brings maps with a better spatial consistency which in some years reachs producers' positive difference close to 7% compared to Collection 7 (Figure 21).

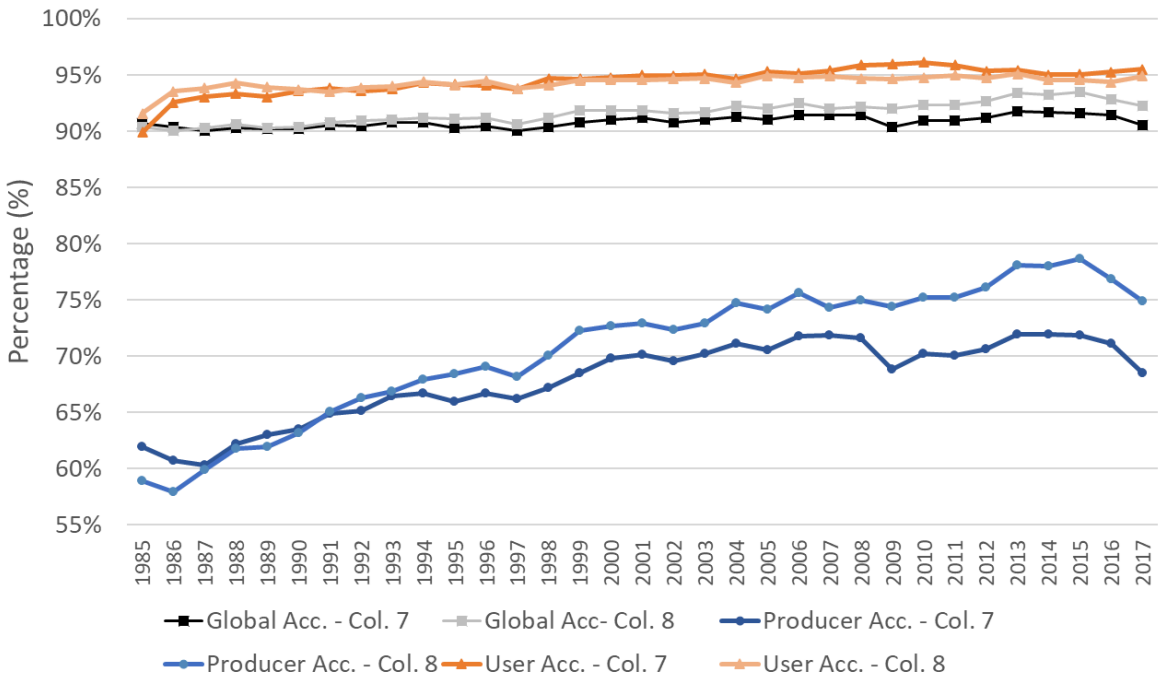

Figure 20. Accuracy assessment (on an annual basis) for Collections 7 and 8, calculated based on the validation samples, only considering points with four or more votes (*i.e.* at least four interpreters identified the same land cover and land use class).

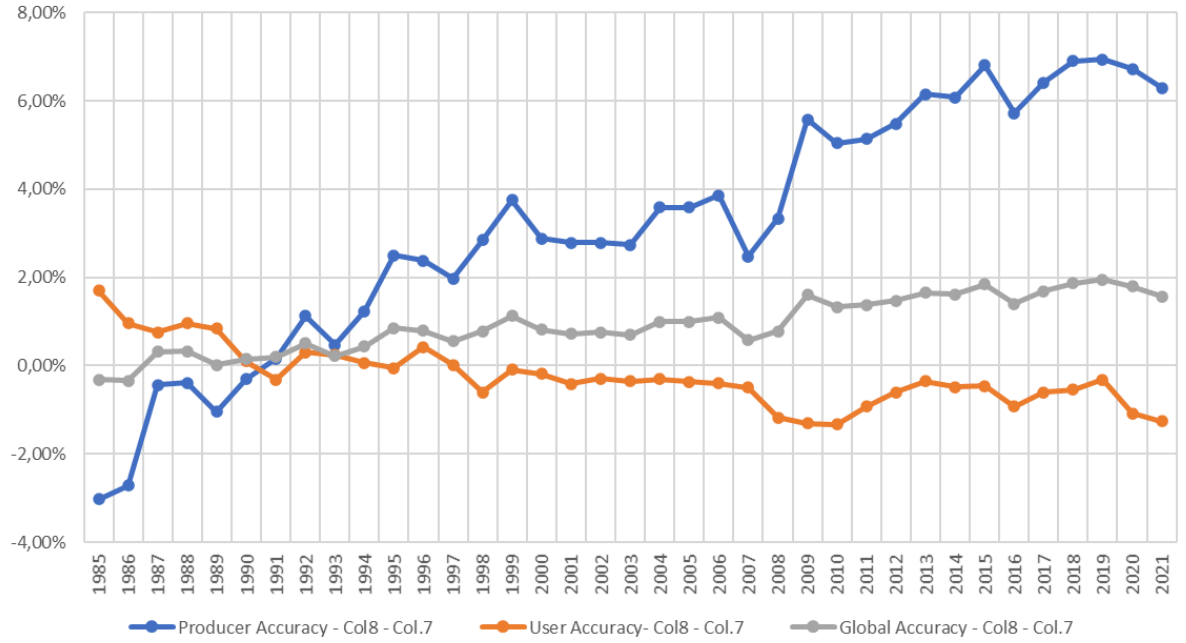

Figure 21. Percentual differences in accuracies between Collections 7 and 8. The revision and increment of new samples, as well as the usage of intervention points, for training the classifier models helped to boost the accuracy values in Collection 8 (at the cost of slightly decreasing the user accuracy).

6.5. Comparison between Collection 8 and 9

No significant differences were observed between collection 8 and 9 (figure 22), with an exception at the beginning of the time series (e.g. 1985 and 1986) where the producer accuracy was lower than Collection 9. Also, a subtle stability is observed in the Collection 9 User Accuracy values.

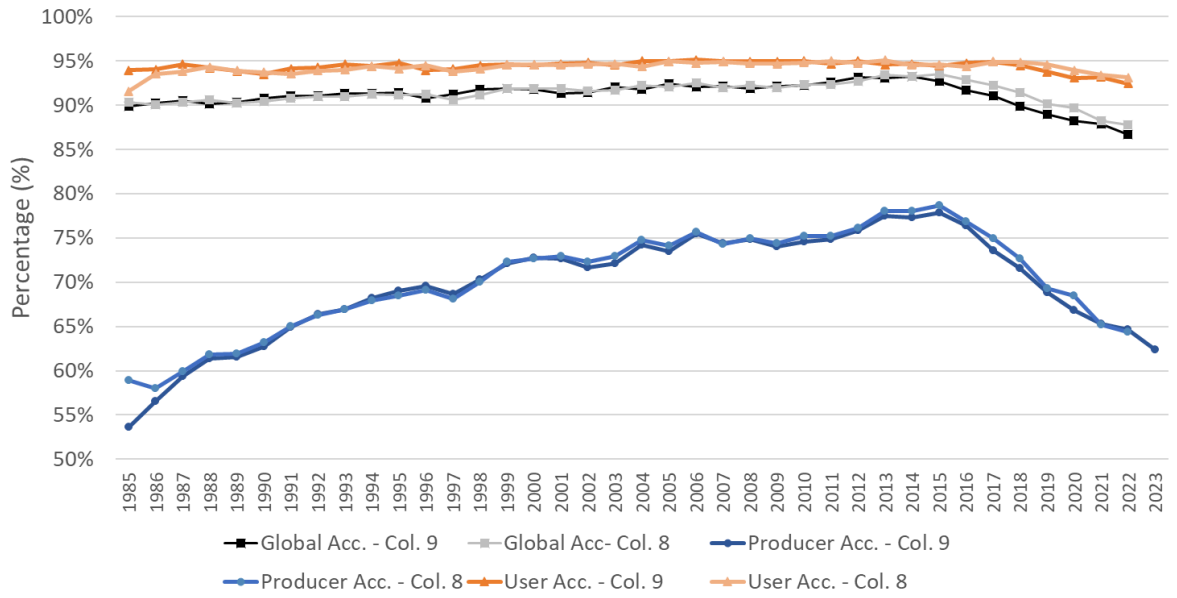

Figure 22. Accuracy assessment (on an annual basis) for Collections 8 and 9, calculated based on the validation samples, only considering points with four or more votes (*i.e.* at least four interpreters identified the same land cover and land use class).

7. Pasture maps integration

For Collection 4, the final pasture area resulted from an integration between Collections 3 and 4 (figure 23); *i.e.* the areas mapped by Collection 4 were considered only in regions mapped with the class Agriculture and Pasture Mosaic (*i.e.* class 21), according to the mapping approach used by the biomes, producing a map with the best aspects of both collections. On the other hand, no integration was considered in Collections 5, 6, and 7.

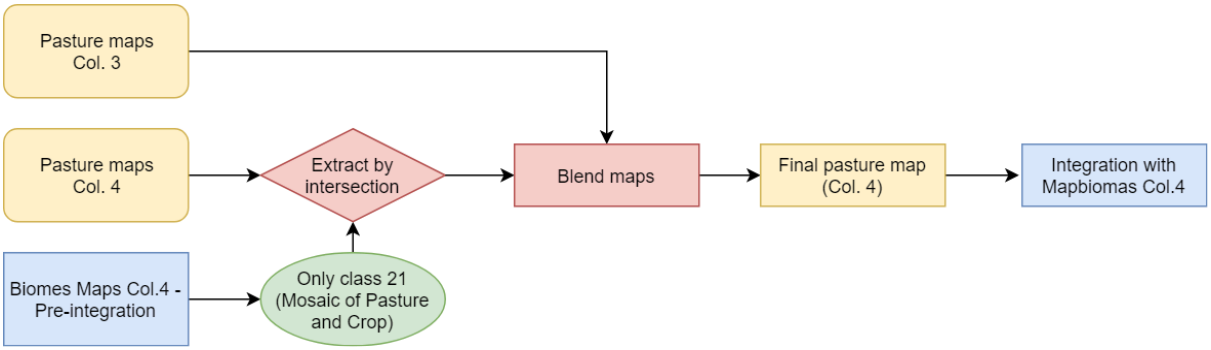

Figure 23. Integration scheme of pasture maps produced in Collection 4.

8. Pasture Quality Mapping

This section presents the progress regarding our pasture vigor condition mapping approach, once called pasture quality.

8.1 *Collection 5*

In Collection 5, the analysis approach for mapping the quality of the Brazilian pastures, considering the years 2010 and 2018, was based on Landsat NDVI images, which functions as a proxy of pasture vigor. Specifically, we followed the method proposed by Gao et al. (2006) with adaptations made by Andrade et al. (2013) for the Brazilian reality.

For the two analyzed periods (*i.e*. 2010 to 2018), NDVI median images within a 24-month time window were used, considering the second semester of the previous year, the year of interest and the first semester of the following year (*e.g*. July / 2009 to June / 2011). To obtain median NDVI images for the beginning and end of the analyzed periods (*i.e*. 2010 to 2018), which were comparable to each other, the following criteria were used:

1 - Equalize the availability of images between sensors (*i.e*. TM and OLI), reducing the data to the monthly average and using only the months with information available for both periods (i.e. 2010 and 2018);

2 - The negative NDVI values were removed from the analysis, since in pasture areas these values tend to be associated with noise in the data;

3 - Landsat 5 data - beginning of the period - were spectral corrected to be compatible with Landsat 8 data - end of the period. The median NDVI images were obtained using all Landsat scenes with less than 80% cloud coverage, and applying the criteria of equalizing the period of the images on a pixel basis.

For each Brazilian biome, the median NDVI images were normalized, using the following equation:

$$NDVIq = \frac{NDVI - NDVImin}{NDVImax - NDVImin}$$

The resultant image corresponds to a pasture condition index, with values between 0 and 1, which was stratified into four categories of pasture quality: not degraded [> 0.6], slightly degraded [0.5 - 0.6], moderately degraded [0.4 - 0.5], and severely degraded [<0.4]). Based on the CAR limits (i.e. Rural Environmental Information concerning property limits), the Pasture Degradation Index was calculated for each Brazilian property, weighting the pasture area in each class of degradation according to the total pasture area on the property (figure 24). For a thorough description of the above strategies and analysis of the results regarding the Collection 5 pasture quality mapping, refer to Santos et al., 2022 paper.

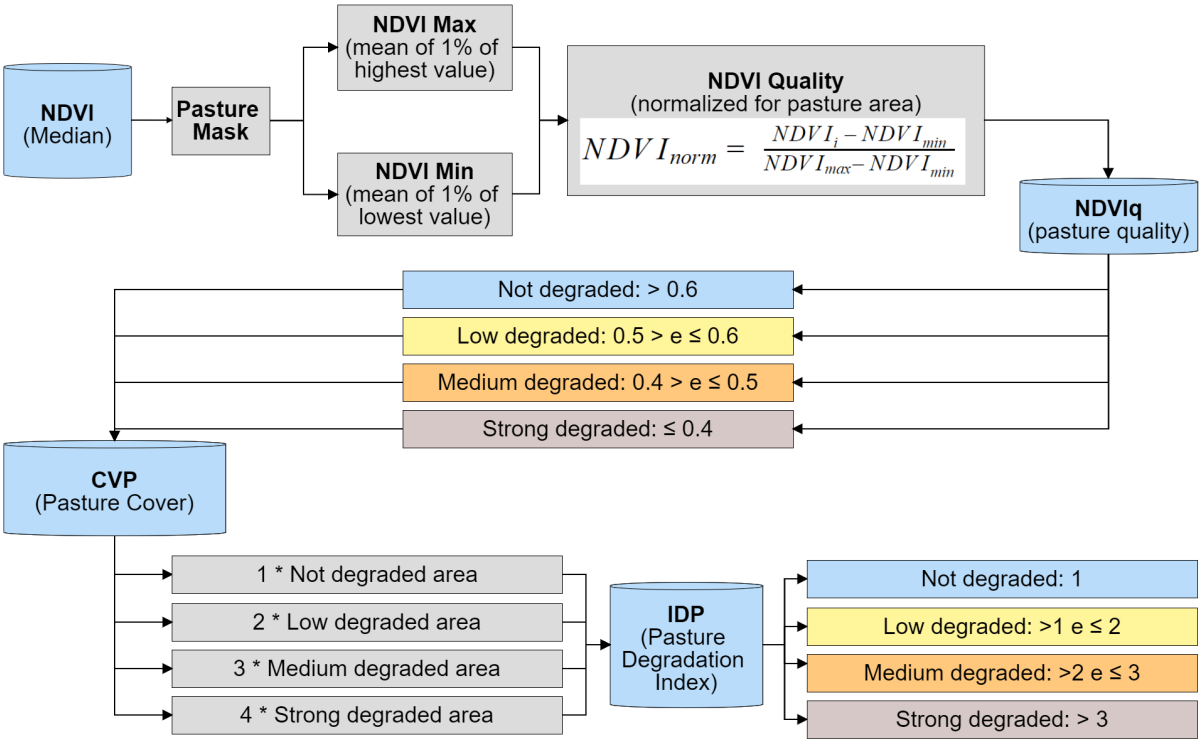

Figure 24. Analysis approach for mapping the quality of the brazilian pasturelands for Collection 5.

8.2 *Collection 6*

To build a consistent pasture quality time series for the entire country, it is necessary to have consistent and stable satellite observations, which are very difficult to obtain based on the regular USGS Landsat archive available via the Google Earth Engine. Thus, for Collection 6 we opted to use the MOD13Q1 EVI data series (2000 to 2020), which were processed with state-of-the-art techniques in order to extract stable (i.e. gap filled series, on a pixel basis, via the use of the TMWM algorithm / code) and seasonally adjusted data (i.e. removal of the seasonal component via the use of the STL algorithm / code). The basic rationale used in Collection 5 was maintained (refer to figure 23), although for each year, the so-called CVP (i.e. pasture vegetative cover - in portuguese) was derived from the normalization of the mean deseasonalized EVI value (from six bi-monthly composites, considering the 90th percentile) and only three quality classes were derived (figure 25).

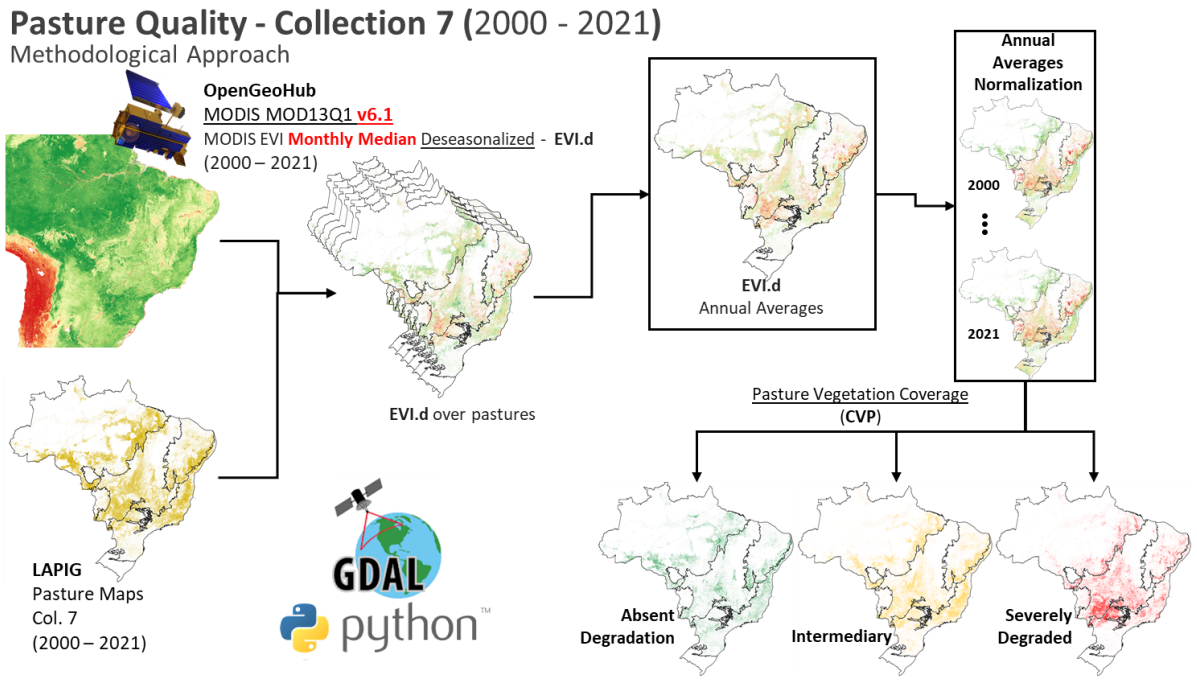

Figure 25. Analysis approach for mapping the quality of the brazilian pasturelands for Collection 7.

8.3 *Collections 7, 8 and 9*

For Collections 7, 8 and 9, our first attempt consisted of using harmonized Landsat ARD images (Analysis Ready Data) made available by the Global Land Analysis and Discovery (GLAD / University of Maryland), whose harmonization strategy enables the generation of radiometrically stable and consistent time series (Potapov et al., 2020). However, in view of the unsatisfactory and not fully understood results, we opted, as in Collection 6 (figure 26), to use MODIS MOD13Q1 images (2000 - 2023). Although the processing logic followed that used for Collection 6, two key modifications were implemented:

1) use of monthly MODIS data (as opposed to bimonthly data);

2) use of the 50th percentile (i.e. median) as opposed to the 90th percentile considered for Collection 6.

These two modifications aimed at more consistent results, while being more conservative in terms of detecting inter-annual variations.

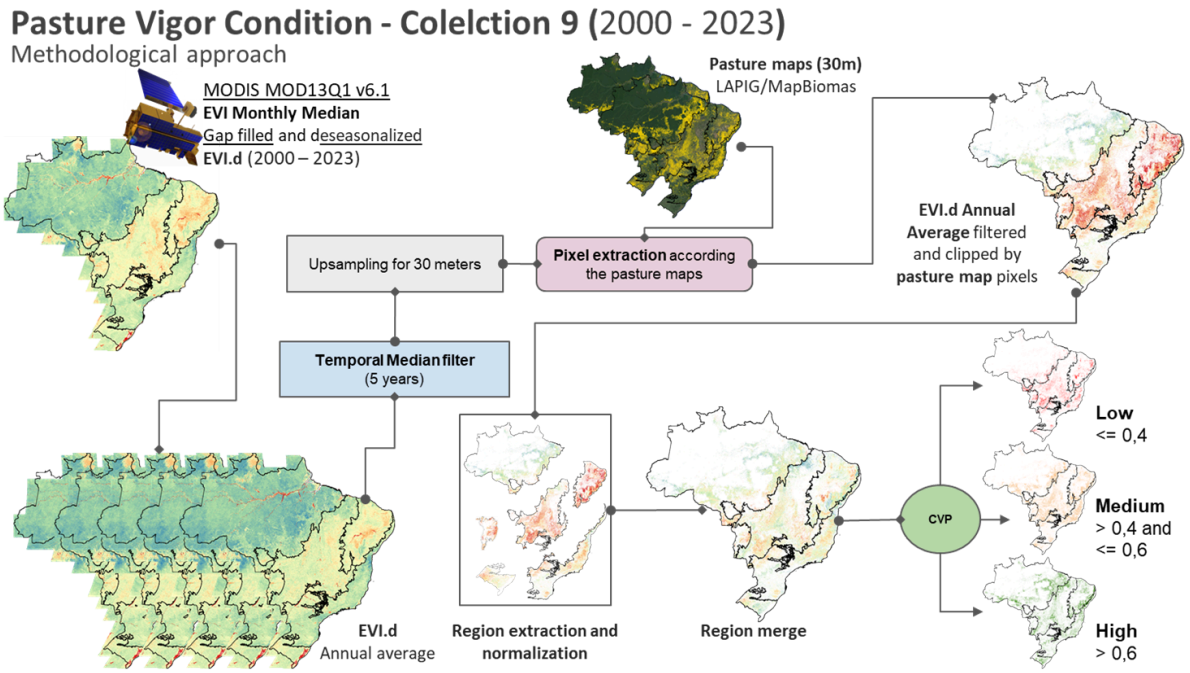

Figure 26. Analysis approach for mapping the vigor of the brazilian pasturelands for Collection 9.

9. Pasture Dry Biomass Productivity mapping approach

This section presents the progress regarding our brand new Pasture Dry Biomass Productivity mapping approach.

9.1 *Collection 9*

Following the steps of Robinson et al. (2018) and Veloso et al. (2020), the Pasture Dry Biomass Productivity maps are based on Gross Primary Productivity (GPP) derived from a light use efficiency model, similar to MODIS MOD17 products, built mainly using remote sensing data. The estimates of GPP (figure 27) follows the formula recommended by Robinson et al. (2018), where the results are the product of the Photosynthetically active radiation (PAR), Absorbed fraction of PAR (fAPAR) and the land cover light use efficiency (LUE).

The PAR estimates used were derived from the Synoptic Radiative Fluxes and Clouds (SYN1deg), which uses Clouds and the Earth's Radiant Energy System (CERES) data in its constitution. For the fAPAR, we consider the bi-monthly gap filled NDVI median based on the harmonized Landsat ARD images (Analysis Ready Data) made by the Global Land Analysis and Discovery (GLAD / University of Maryland), which delivers a stable time series. Specific for the LUE estimates, a standard value of 0,5 gC/m²/day was used for the Brazilian pasturelands, as recommended by the work of Veloso et al. (2020). Also, to make the LUE information more realistic, an adjustment using a temperature and wetness scalar was used, estimates using bi-monthly MODIS MOD11 gap filled and NDWI from Landsat ARD data. The conversion of GPP to Dry Biomass was made using a conversion factor of 1,62, which converts gC/m²/day to tons of dry biomass/ha/year.

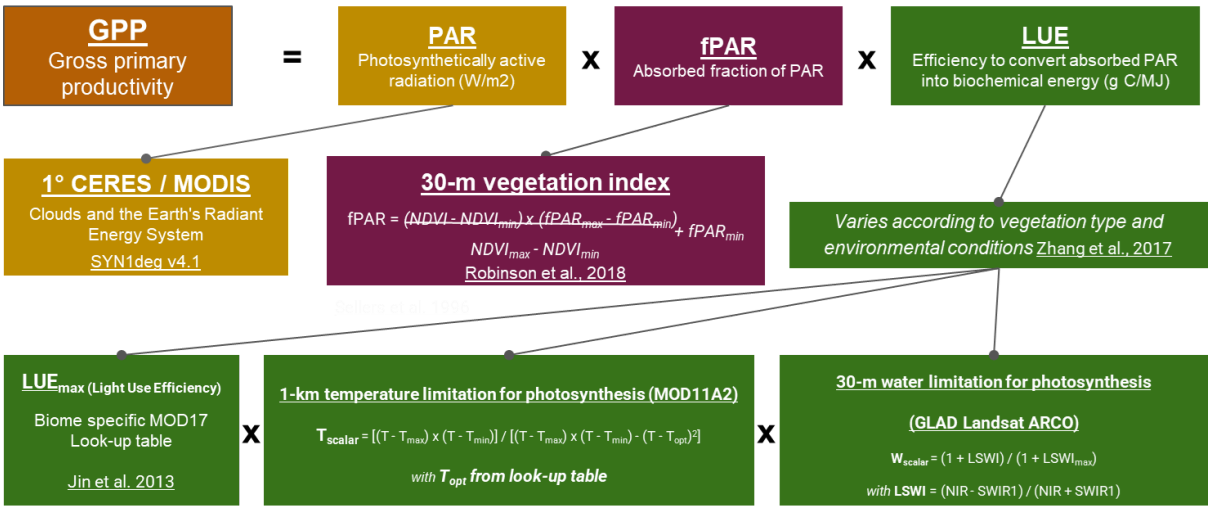

Figure 27. Workflow used to estimate GPP based on Robinson *et al.* (2018) and Veloso *et al.* (2020) approaches.

10. References

AGUIAR, D. A.; MELLO, M. P.; NOGUEIRA, S. F.; GONÇALVES, F. G.; ADAMI, M.; RUDORFF, B. T. MODIS time series to detect anthropogenic interventions and degradation processes in tropical pasture. Remote Sensing, v. 9, n. 1, p. 73, 2017.

ANDRADE, R.G., RODRIGUES, C.A.G., SANCHES, I.D.A., TERRESAN, F.E., QUARTORALI, C.F.. Uso de técnicas de sensoriamento remoto na detecção de processos de degradação de pastagens. Revista Engenharia na Agricultura-Reveng, v.21, n.3, p.234-243, 2013.

BREIMAN, L. Random forests. Machine learning, v. 45, n. 1, p. 5-32, 2001.

CARET. Model Training and Tuning. Available online: http://topepo.github.io/caret/model-training-and-tuning.html#model-training-and-parameter-tuning (accessed on 27 August 2020).

CHAVEZ JR., P.S ; MACKINNON, D.J. Automatic detection of vegetation changes in the southwestern United States using remotely sensed images, Photogrammetric Engineering and Remote Sensing, v. 60, pp. 571-583, 1994.

FARR, T. G., *et al*. The Shuttle Radar Topography Mission, Rev. Geophys., V45, 2007.

FERREIRA, L. G.; SANO, E. E.; FERNANDEZ, L. E.; ARAÚJO, F. M. Biophysical characteristics and fire occurrence of cultivated pastures in the Brazilian savanna observed by moderate resolution satellite data. International journal of remote sensing, v. 34, n. 1, p. 154-167, 2013.

FERREIRA, L. G.; FERNANDEZ, L. E.; SANO, E. E.; FIELD, C.; SOUSA, S. B.; ARANTES, A. E.; ARAÚJO, F. M. Biophysical properties of cultivated pastures in the Brazilian savanna biome: An analysis in the spatial-temporal domains based on ground and satellite data. Remote Sensing, v. 5, n. 1, p. 307-326, 2013b.

FURBY, S. L.; CAMPBELL, N. A. Calibrating images from different dates to 'like-value'digital counts. Remote Sensing of Environment, v. 77, n. 2, p. 186-196, 2001.

GAO, B.C. NDWI – A Normalized Difference Water Index for remote sensing of vegetation liquid water from space. Remote Sensing of Environment, v.58, p.257-266, 1996.

KUHN, M. Building Predictive Models in R Using the caret Package. Journal of Statistical Software, v. 28, n. 5,p. 1 - 26, 2008

LIAW, A.; WIENER, M. Classification and Regression by randomForest. R News. v. 2, n. 3, p. 18-22, 2002 (available online: https://cran.r-project.org/web/packages/randomForest/index.html)

LOHR, S.L. Sampling: Design and Analysis, 2 edition. ed. Cengage Learning, Boston, Mass, 2009.

MARKHAM, B. L.; HELDER, D. L. Forty-year calibrated record of earth-reflected radiance from Landsat: A review. Remote Sensing of Environment, v. 122, p. 30-40, 2012.

MARKHAM, B. L.; STOREY, J. C.; WILLIAMS, D. L.; IRONS, J. R. Landsat sensor performance: history and current status. Geoscience and Remote Sensing, IEEE Transactions on, v. 42, n. 12, p. 2691-2694, 2004.

NAGLER, P. L.; INOUE, Y.; CLENN, E. P.; RUSS, A. L.; DAUGHTRY, C. S. T. Cellulose absorption index (CAI) to quantify mixed soil-plant litter scenes. Remote Sens Environ, v. 87, pp. 310–325, 2003.

NOGUEIRA, S.; PARENTE, L.; FERREIRA, L. Temporal Visual Inspection: Uma ferramenta destinada à inspeção visual de pontos em séries históricas de imagens de sensoriamento remoto. In XXVII Congresso Brasileiro de Cartografia; Instituto Brasileiro de Geografia e Estatística: Rio de Janeiro, Brazil, 2017.

PARENTE, L.L., SILVA, A.P., BAUMANN, L.F., LOPES, V., SILVA, E.B., NOGUEIRA, S., MESQUITA, V.V., FERREIRA, L.G. Shaping the Brazilian landscape: a process drive by land occupation, large-scale deforestation, and rapid agricultural expansion. Scientific Reports, 2021 (preprint available at Research Square).

PARENTE, L.L., MESQUITA, V.V., MIZIARA, F., BAUMANN, L.F., FERREIRA, L.G. Assessing the pasturelands and livestock dynamics in Brazil, from 1985 to 2017: A novel approach based on high spatial resolution imagery and Google Earth Engine cloud computing. Remote Sensing of Environment, v. 232, p. 111301, 2019.

PARENTE, L.; FERREIRA, L.. Assessing the Spatial and Occupation Dynamics of the Brazilian Pasturelands Based on the Automated Classification of MODIS Images from 2000 to 2016. Remote Sensing, v. 10, n. 4, p. 606, 2018.

PARENTE, L.; FERREIRA, L.; FARIA, A.; NOGUEIRA, S.; ARAÚJO, F.; TEIXEIRA, L.; HAGEN, S. Monitoring the brazilian pasturelands: A new mapping approach based on the landsat 8 spectral and temporal domains. International Journal of Applied Earth Observation and Geoinformation, v. 62, p. 135-143, 2017.

PASQUARELLA, V. J.; HOLDEN, C. E.; WOODCOCK, C. E. Improved mapping of forest type using spectral-temporal Landsat features. Remote Sensing of Environment, v. 210, p. 193-207, 2018.

PONTIUS JR, R. G.; & MILLONES, M. Death to Kappa: birth of quantity disagreement and allocation disagreement for accuracy assessment. International Journal of Remote Sensing, v. 32, n. 15, p. 4407-4429, 2011.

POTAPOV, P., HANSEN, M.C., KOMMAREDDY, I., KOMMAREDDY, A., TURUBANOVA, S., PICKENS, A., ADUSEI, B., TYUKAVINA, A., YING, Q. Landsat Analysis Ready Data for Global Land Cover and Land Cover Change Mapping. Remote Sensing, 12, 426-448, 2020.

R Core Team. R: A language and environment for statistical computing. R Foundation for Statistical Computing, Vienna, Austria, 2020. Available online: https://www.R-project.org/

ROY, D.P.; WULDER, M.A.; LOVELAND, T.R.; WOODCOCK, C.E; ALLEN, R.G.; ANDERSON, M.C.; HELDER, D.; IRONS, J.R.; JOHNSON, D.M.; KENNEDY, R.; SCAMBOS, T.A.; SCHAAF, C.B.; SCHOTT, J.R.; SHENG, Y.; VERMOTE, E.F.; BELWARD, A.S.; BINDSCHADLER, R.; COHEN, W.B.; GAO, F.; HIPPLE, J.D.; HOSTERT, P.; HUNTINGTON, J.; JUSTICE, C.O.; KILIC, A.; KOVALSKYY, V.;

LEE, Z.P.; LYMBURNER, L.; MASEK, J.G.; MCCORKEL, J.; SHUAI, Y.; TREZZA, R.; VOGELMANN, J.; WYNNE, R.H.; ZHU, Z. Landsat-8: Science and product vision for terrestrial global change research. Remote sensing of Environment, v. 145, p. 154-172, 2014.

ROY, D.P.; KOVALSKYY, V.; ZHANG, H.K.; VERMOTE , E.F.; YAN, L.; KUMAR, S.S.; EGOROV, A. Characterization of Landsat-7 to Landsat-8 reflective wavelength and normalized difference vegetation index continuity, Remote Sensing of Environment, Volume 185, pp. 57-70, 2016.

ROBINSON, N. P. et al. Terrestrial primary production for the conterminous United States derived from Landsat 30 m and MODIS 250 m. Remote Sensing in Ecology and Conservation, v. 4, n. 3, p. 264–280, 2 mar. 2018.

SANTOS, CLAUDINEI OLIVEIRA DOS ; MESQUITA, VINÍCIUS VIEIRA ; PARENTE, LEANDRO LEAL ; PINTO, ALEXANDRE DE SIQUEIRA ; FERREIRA, LAERTE GUIMARAES FERREIRA . Assessing the Wall-to-Wall Spatial and Qualitative Dynamics of the Brazilian Pasturelands 2010-2018, Based on the Analysis of the Landsat Data Archive. Remote Sensing, v. 14, p. 1024-1039, 2022.

SCIPY. Reference Guide - SciPy v1.1.0. Available online: https://docs.scipy.org/doc/scipy-1.1.0/reference/generated/scipy.ndimage.median.html (accessed on 01 August 2018).

VELOSO, G. A. et al. Modelling gross primary productivity in tropical savanna pasturelands for livestock intensification in Brazil. Remote Sensing Applications: Society and Environment, v. 17, p. 100288, jan. 2020.

WANG, J.; ZHAO, Y.; LI, C.; YU, L.; LIU, D.; GONG, P. Mapping global land cover in 2001 and 2010 with spatial-temporal consistency at 250 m resolution. ISPRS Journal of Photogrammetry and Remote Sensing, v. 103, p. 38-47, 2015.

ZALLES, VIVIANA; HANSEN, MATTHEW C.; POTAPOV, PETER V.; STEHMAN, STEPHEN V.; TYUKAVINA, ALEXANDRA; PICKENS, AMY; SONG, XIAO-PENG; ADUSEI, BERNARD; OKPA, CHIMA; AGUILAR, RICARDO; JOHN, NICHOLAS; CHAVEZ, SELENA. Near doubling of Brazil's intensive row crop area since 2000. Proceedings of the National Academy of Sciences of the United States of America, v.116, n. 2, p. 428-435, 2019.